

A micro methanol fuel cell operating at near room temperature

T. J. Yen, N. Fang, X. Zhang, G. Q. Lu, and C. Y. Wang

Citation: *Applied Physics Letters* **83**, 4056 (2003); doi: 10.1063/1.1625429

View online: <http://dx.doi.org/10.1063/1.1625429>

View Table of Contents: <http://scitation.aip.org/content/aip/journal/apl/83/19?ver=pdfcov>

Published by the [AIP Publishing](#)

Articles you may be interested in

[Synthesis and characterization of proton conducting inorganic-organic hybrid nanocomposite films from mixed phosphotungstic acid/phosphomolybdic acid/tetramethoxysilane/3-glycidoxypropyltrimethoxysilane/phosphoric acid for H₂ / O₂ fuel cells](#)

J. Renewable Sustainable Energy **1**, 063106 (2009); 10.1063/1.3278517

[Performance comparison between planar and tubular-shaped ambient air-breathing polymer electrolyte membrane fuel cells using three-dimensional computational fluid dynamics models](#)

J. Renewable Sustainable Energy **1**, 023105 (2009); 10.1063/1.3114443

[Platinum/multiwalled carbon nanotubes-platinum/carbon composites as electrocatalysts for oxygen reduction reaction in proton exchange membrane fuel cell](#)

Appl. Phys. Lett. **88**, 253105 (2006); 10.1063/1.2214139

[Nanostructured tungsten carbide catalysts for polymer electrolyte fuel cells](#)

Appl. Phys. Lett. **86**, 224104 (2005); 10.1063/1.1941473

[Tree network channels as fluid distributors constructing double-staircase polymer electrolyte fuel cells](#)

J. Appl. Phys. **96**, 842 (2004); 10.1063/1.1757028



A micro methanol fuel cell operating at near room temperature

T. J. Yen, N. Fang, and X. Zhang^{a)}

Department of Mechanical and Aerospace Engineering, University of California at Los Angeles, 420 Westwood Plaza, Los Angeles, California 90095

G. Q. Lu and C. Y. Wang

Electrochemical Engine Center (ECEC), and Department of Mechanical and Nuclear Engineering, the Pennsylvania State University, University Park, Pennsylvania 16802

(Received 18 July 2003; accepted 16 September 2003)

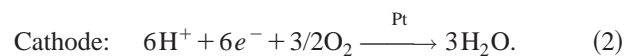
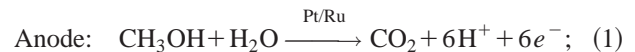
We present a bipolar micro direct methanol fuel cell (μ DMFC) with high-power density and simple device structure. A proton exchange membrane-electrode assembly was integrated in a Si-based μ DMFC with micro channels 750 μ m wide and 400 μ m deep, fabricated using silicon micromachining. The μ DMFC has been characterized at near room temperature, showing a maximum power density of 47.2 mW/cm² when 1 M methanol was fed at 60 °C. The cell voltage dependence on the current density agrees well with the modified Tafel model, in which regimes of kinetic polarization and ohmic polarization are observed without significant presence of the concentration polarization. © 2003 American Institute of Physics. [DOI: 10.1063/1.1625429]

To enable the future multifunctional, high-performance microelectronic devices and microelectromechanical systems (MEMS), it is critical to develop compact and high-efficiency micro power sources. Recent developments in micro turbine engines and other types of combustion-based micro devices represent an important step towards micro power sources. The critical challenges of these devices often are associated with complex high-speed machinery with very tight tolerance, toxic emissions, and high-temperature-resistant materials systems.¹ Recently, the miniaturization of fuel cells²⁻⁴ has drawn significant interest because of potential advantages such as high-energy density, low operating temperature, environmental-friendly emissions, and the potential to eliminate moving parts. Among the diverse micro fuel cells,⁵ the polymer electrolyte membrane fuel cell (PEMFC)⁶⁻⁸ offers the advantages of a compact package and operation near room temperature. In a PEMFC, hydrogen and methanol are the common fuels. Miniaturizing a hydrogen fuel cell,⁶ however, suffers a significant limitation of hydrogen storage.⁹ A micro direct methanol fuel cell (μ DMFC), therefore, emerges as one of the favorable candidates for portable electronic communication and computing devices as well as for implantable medical tools.

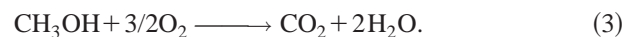
In a μ DMFC, miniaturized channel design impacts the performance of the fuel circulation for ensuring laminar flow at the electrodes, increasing the surface area to volume ratio, and augmenting the yield of desired chemical products.¹⁰ The advancement of silicon MEMS technology enables on-chip integration of these compact microchannel structures for microfluidic systems,¹¹ with precise and reproducible fabrication. In this letter, we present a silicon-based bipolar μ DMFC operating near room temperature.

Figure 1 shows the working principle¹² of an operating μ DMFC. An aqueous methanol solution is fed into the anode, where methanol reacts electrochemically with water to

produce electrons, protons, and carbon dioxide. The electrons produced at the anode carrying the free energy charge of the chemical reaction are forced to flow through an external circuit to deliver electrical work, whereas the protons can migrate through a proton exchange membrane to the cathode, where they combine with oxygen from air and electrons coming back from the external circuit to form water:



The overall reaction can be expressed by



Intuitively, the higher the methanol concentration in the fuel cell, the more protons it can supply, producing higher current. However, under the condition of high methanol concentration, the methanol crosses over the proton-diffusion membrane from the anode to the cathode, which can drasti-

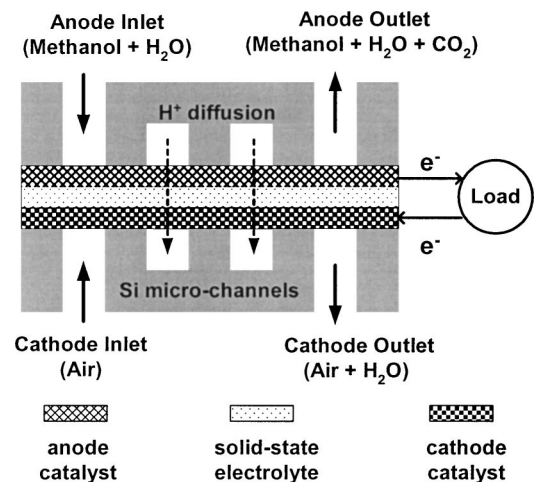


FIG. 1. Illustration of a methanol fueled μ DMFC element. The rationale to operate this fuel cell can be interpreted by the anodic and cathodic half-reactions.

^{a)}Author to whom correspondence should be addressed; electronic mail: xiang@seas.ucla.edu

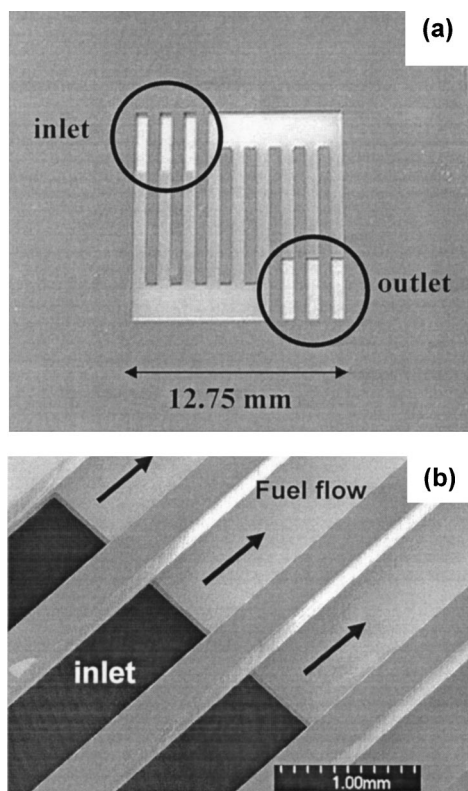


FIG. 2. (a) Optical image of the Si-based bipolar plate. The detailed dimensions of the serpentine flowfield are $750\ \mu\text{m}$ in width, $400\ \mu\text{m}$ in depth, and $12.75\ \text{mm}$ in length. (b) SEM image at the tubing area. It shows details of the channels, exhibiting the well-defined geometrical structure by two DRIE processes.

cally poison the electrodes. In this case, methanol directly reacts with oxygen at the cathode and generates no current, reducing energy conversion efficiency. Considering the trade-off between supplying enough protons and avoiding methanol poisoning, we chose 1 M methanol solution to test the performance of the μDMFC .

The μDMFC is fabricated by silicon micromachining. A pair of $500 \pm 20\ \mu\text{m}$ silicon wafers is employed as bipolar plates. On top of each half-plate, we patterned the serpentine channels with three parallel partial cross sections to mitigate the clogging of byproduct CO_2 in the flow field. Deep reactive ion etching (DRIE) is applied to anisotropically inscribe fluid channels into Si wafers with $400\ \mu\text{m}$ in depth. Next, double-sided alignment photolithography is conducted to pattern the back side of the wafers to form fuel feeding holes. Another DRIE step is followed to fabricate through-hole structures, allowing methanol fuel to flow in and out. Ti/Cu/Au ($0.01/3/0.5\ \mu\text{m}$) layers are then deposited on the front side of the wafers by electron-beam evaporation in order to collect the generated current. This rugged electrode is proposed to increase the diffusion current density j_0 up to two times compared to the planar electrode configuration.¹³ Ultimately, a home-made membrane electrode assembly (MEA) is sandwiched between the bipolar plates to create an integrated μDMFC , as shown in Fig. 1. Figure 2(a) represents the optical micrograph of the bipolar plates. The dimensions of channels and ribs are $750\ \mu\text{m}$ wide and $12.75\ \text{mm}$ long, which comprise an effective cell area of $1.625\ \text{cm}^2$. Figure 2(b) shows the scanning electron microscope (SEM) picture of the channels and inlet of the micro fuel cell, exhibiting the

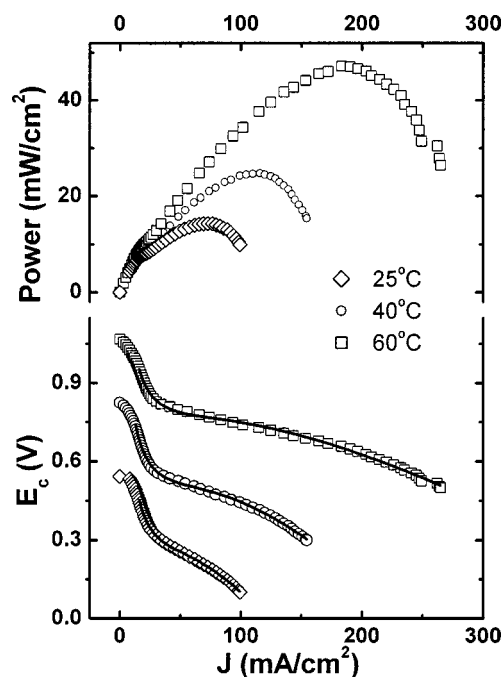


FIG. 3. Cell performance curves at 23, 40, and $60\ ^\circ\text{C}$ at ambient pressure. In the lower panel, the current polarization curves are offset by $0.2\ \text{V}$ for $40\ ^\circ\text{C}$, and $0.4\ \text{V}$ for $60\ ^\circ\text{C}$, for clarity. The 1 M methanol solution was employed with the flow rate of $0.283\ \text{mL/min}$, and the air flow rate is $88\ \text{mL/min}$. The solid lines in the lower panel are fitted using modified Tafel equation (see Refs. 15 and 16).

well-defined vertical wall of ribs and channels. The MEA is the central component for the electrochemical energy conversion, which not only contains two porous electrodes to efficiently activate electrochemical half-reactions, but also an embedded solid-state electrolyte to conduct protons. To produce a home-made MEA, a Nafion 112 (EW 1100, Dupont) membrane was sandwiched between the anode and cathode.¹⁴ First, the Nafion 112 membrane was processed by hydrogen peroxide aqueous solution (5 wt%) at $80\ ^\circ\text{C}$, followed by immersion in distilled water, then immersed in sulfuric acid aqueous solution (1 M) at $80\ ^\circ\text{C}$, followed by a final immersion in distilled water. Each of these chemical treatments and rinsing procedures takes a period of 2 h. Finally, the anode layer, the treated Nafion 112 membrane, and the cathode layer were hot pressed at $125\ ^\circ\text{C}$ at a pressure of $100\ \text{kg/cm}^2$ for 3 min to form the MEA structure.

To measure the cell performance, we utilized a peristaltic pump to deliver the liquid fuel (1 M aqueous methanol), with a feeding rate of $0.283\ \text{mL/min}$. A gas flow meter was also equipped to monitor an $88\ \text{mL/min}$ air flow at room temperature. Meanwhile, an electric heater with temperature control was attached to the surface of the cell to investigate the cell output at different temperatures. An electronic load system (BT4, Arbin) was utilized to measure the relationship between cell voltage and current density (termed as polarization curve) in a galvanodynamic polarization mode at a scan rate of $3\ \text{mA/s}$.

The open-circuit cell polarization curves at different temperatures are presented in Fig. 3, measured under ambient pressure. As shown in the upper panel of Fig. 3, the maximum power density attains $14.3\ \text{mW/cm}^2$ at $23\ ^\circ\text{C}$, $24.8\ \text{mW/cm}^2$ at $40\ ^\circ\text{C}$, and $47.2\ \text{mW/cm}^2$ at $60\ ^\circ\text{C}$. The output power increases at elevated temperature due to the activation

of a catalyst that reduces the overpotential loss, thus improving the efficiency of electrochemical reaction. The power density of 47 mW/cm² at 60 °C is among the highest densities achieved today in a micro fuel cell, and is comparable to the micro hydrogen fuel cell (40 mW/cm² at 90 °C).^{6,8}

Associated with the electrochemical process described by Eqs. (1)–(3), the relation between cell potential E_c and the current density j can be simplified as the Tafel equation:¹²

$$E_c = E_r - b \log(j/j_0) - j \cdot r, \quad (4)$$

where E_r is reversible potential of the cell (1.18 V at 25 °C), j_0 the exchange current density for oxygen reduction, r the area specific ohmic resistance, and the Tafel slope b , defined as $b = k_B T / (2e\beta)$. Here, k_B is the Boltzmann constant, e the electron charge, T the operating temperature (in K), and β the transfer coefficient determined by the catalyst.

From Eq. (4), the cell voltage drops logarithmically at low current density, which is dubbed “kinetic polarization” and is related to the energy barrier that must be overcome to initiate a chemical reaction between reactants. With increasing current density, the regime named “ohmic polarization” arises due to resistive losses in the cell; for example, within the electrolyte (ionic), in the electrodes (electronic and ionic), and in the terminal connections in the cell (electronic). In practical fuel cells, the mass transport limitation of fuels, oxygen, and byproducts (water and CO₂) leads to a modified Tafel equation by adding an empirical term $C_1 \log(1 - C_2 j)$,^{15,16} in which C_1 and C_2 are fitting parameters.

From the lower panel of Fig. 3, the regimes of kinetic and ohmic polarization are observed in our μ DMFC, typical characteristics of most macroscale DMFCs. A simple data fit using Eq. (4) yields a Tafel slope of 0.214 V at 60 °C and an ohmic resistance of 0.46 Ω cm²; however, the fitting leads to a deviation when cell potential is below 0.2 V. Instead, when using the modified Tafel model, the fitted curves (solid lines in the lower panel) for all three temperature conditions are in good agreement with the experimental results. The fitting parameters are $C_1 = -2.40$, -1.94 , and -1.12 V; and $C_2 = -25.5$, -18.4 , and -36.5 cm²/A for 23, 40, and 60 °C, respectively. Therefore, the experimental results suggest a possible mass transport limitation. However, our bipolar μ DMFC does not display a dramatic voltage drop at 200–300 mA/cm²; that is, a typical fuel concentration polarization, which usually results from the depletion of fuel supply

at the anode. Our prior work on macro methanol fuel cells instead indicates a remarkable contribution of cathode flooding,¹⁷ especially at high current density. This can be optimized in the future by increasing the air flow rate and reducing cathode exit pressure.

In conclusion, we designed and fabricated a silicon-based bipolar micro direct methanol fuel cell using MEMS technology. The performance of the μ DMFC was characterized at near room temperature by using 1 M methanol solution at ambient pressure. Integrating the home-made MEA between a pair of Si-based microchannels to form a bipolar μ DMFC, the maximum output power density is 47.2 mW/cm² at 60 °C and 14.3 mW/cm² at room temperature. The silicon microfabrication of the fuel cells demonstrated the potential to provide an efficient power source for portable electronic devices and MEMS.

This work is supported by DARPA Microsystem Technology Office under Contract No. DAAH01-1-R001.

- ¹A. Mehra, X. Zhang, A. A. Ayon, I. A. Waitz, M. A. Schmidt, and C. M. Spadaccini, *J. Microelectromech. Syst.* **9**, 517 (2000).
- ²S. R. Narayanan and T. I. Valdez, in *Handbook of Fuel Cells—Fundamentals, Technology and Application*, edited by W. Vielstich, A. Lamm, and H. A. Gasteiger (Wiley, Hoboken, NJ, 2003), Vol. 4, p. 1133.
- ³C. Bailey, *Proceedings of the Conference on Advances in R&D for the Commercialization of Small Fuel Cells and Battery Technologies for Use in Portable Application*, 29 April, 1999, Bethesda, MD.
- ⁴C. K. Dyer, *J. Power Sources* **106**, 31 (2002).
- ⁵B. C. H. Steele and A. Heinzel, *Nature (London)* **414**, 345 (2001).
- ⁶S. J. Lee, A. Chang-Chien, S. W. Cha, R. O’Hayre, Y. I. Park, Y. Saito, and F. B. Prinz, *J. Power Sources* **112**, 410 (2002).
- ⁷A. Heinzel, C. Hebling, M. Muller, M. Zedda, and C. Muller, *J. Power Sources* **105**, 250 (2002).
- ⁸S. C. Kelley, G. A. Deluga, and W. H. Smyrl, *Electrochem. Solid-State Lett.* **3**, 407 (2000).
- ⁹L. A. Züttel, *Nature (London)* **414**, 353 (2001).
- ¹⁰H. L. Maynard and J. P. Meyers, *J. Vac. Sci. Technol. B* **20**, 1287 (2002).
- ¹¹S. Terry, J. Jenman, and J. Angell, *IEEE Trans. Electron Devices* **ED-26**, 1880 (1979).
- ¹²*Fuel Technology Handbook*, edited by G. Hoogers (CRC Press, Boca Raton, FL, 2003), Chaps. 3, 4, and 7.
- ¹³Y. H. Seo and Y.-H. Cho, *Proceedings of IEEE MEMS 2003*, Kyoto (IEEE, New York, 2003), p. 375.
- ¹⁴G. Q. Lu, T. J. Yen, X. Zhang, and C. Y. Wang, *Electrochim. Acta* (to be published).
- ¹⁵G. Squadrito, G. Maggio, E. Passalacqua, F. Lufrano, and A. Patti, *J. Appl. Electrochem.* **29**, 1449 (1999).
- ¹⁶P. Argyropoulos, K. Scott, A. K. Shukla, and C. Jackson, *Fuel Cells* **2**, 78 (2002).
- ¹⁷M. M. Mench, S. Boslet, S. Thynell, J. Scott, and C. Y. Wang, *Proceedings of the International Symposium on Direct Methanol Fuel Cells*, 2001 (Electrochemical Society, Pennington, NJ, 2001), Vol. 2001-4, p. 241.